International Journal of Energy Production and Management
https://www.acadlore.com/journals/IJEPM

The Effect of Cover Cooling and Solar Collector Integration on the Productivity of a Double-Slope Solar Still

Wando Simanullang[1], Yogie Probo Sibagariang[2], Tulus Burhanuddin Sitorus[1], Himsar Ambarita[1*], Hendrik Voice Sihombing[1], Yoshihiko Oishi[3]

[1] Department of Mechanical Engineering, Universitas Sumatera Utara, 20155 Medan City, Indonesia
[2] Research Center for Energy Conversion and Conservation, National Research and Innovation Agency (BRIN), 10340 Jakarta, Indonesia
[3] Division of Production Systems Engineering, Muroran Institute of Technology, 050-8585 Muroran, Japan

[*] Correspondence: Himsar Ambarita (himsar@usu.ac.id)

Received: 08-11-2025 **Revised:** 10-04-2025 **Accepted:** 10-08-2025

Citation: W. Simanullang, Y. P. Sibagariang, T. B. Sitorus, H. Ambarita, H. V. Sihombing, and Y. Oishi, "The effect of cover cooling and solar collector integration on the productivity of a double-slope solar still," *Int. J. Energy Prod. Manag.*, vol. 10, no. 3, pp. 420–435, 2025. https://doi.org/10.56578/ijepm100306.

Abstract: While solar still technology offers a sustainable solution to freshwater scarcity, its practical application is often limited by low productivity. This study aims to enhance the water production of a double-slope solar still through the simultaneous implementation of a glass cover cooling mechanism and a flat-plate solar collector. Three configurations were experimentally compared: a conventional solar still (SSC), a solar still with cover cooling (SST1), and a solar still integrating both cover cooling and a solar collector (SST2). Experimental results show that SST2 achieved lower glass cover temperatures than the SSC and higher water temperatures than the SST1, thereby accelerating both evaporation and condensation rates. Quantitatively, the SST2 configuration yielded a freshwater productivity of 2092 g/m^2, a significant increase of 147% compared to the SSC. Furthermore, its energy efficiency reached 44.53%, in contrast to 27.38% for SSC and 27.27% for SST1. Economically, SST2 demonstrated the lowest freshwater production cost at \$0.082/(L·m^2). These findings rigorously prove that the simultaneous use of cover cooling and a solar collector is a highly effective strategy for increasing the productivity and improving the economic viability of solar stills.

Keywords: Solar still; Cooling, Solar collector; Energy analysis; Economic analysis

1 Introduction

Fresh water is essential for all living organisms, yet it remains a scarce resource in many developing countries. The World Health Organization (WHO) estimates that due to population growth and climate change, approximately 2 billion individuals lack access to safe drinking water [1]. Of all water on Earth, only 3% is fresh water, with the remaining 97% being saline ocean water [2, 3]. One viable alternative for addressing this scarcity is solar still technology, which uses solar energy to produce clean water from seawater and other non-potable sources [4].

Despite their simple construction, conventional solar stills (SSCs) suffer from inherently low freshwater productivity. Performance is influenced by external factors, such as cloud cover, and internal factors, including water depth, absorber plate material, and the critical processes of evaporation and condensation [5, 6]. The rates of these two processes are paramount; evaporation is accelerated by higher water temperatures, while condensation is enhanced by lower glass cover temperatures.

This challenge is particularly relevant in equatorial nations like Indonesia, which possess abundant solar radiation year-round. While this potential has spurred research into various solar applications, such as hybrid power systems for electric vehicle charging stations [7]. A primary barrier to widespread adoption remains the high upfront investment cost. This economic constraint underscores the importance of developing and optimizing cost-effective and highly efficient systems, such as the enhanced solar still investigated in this study.

Therefore, this study aims to improve the productivity of a double-slope solar still by simultaneously implementing a glass cover cooling mechanism and a flat-plate solar collector. Three configurations were experimentally tested and

analyzed for their thermal characteristics, freshwater productivity, energy efficiency, and economic viability. The experimental findings revealed that the solar still integrating both cover cooling and a solar collector (SST2) resulted in a substantial performance improvement, increasing freshwater productivity by 147% and achieving an energy efficiency of 44.53% compared to SSCs. Consequently, the SST2 model also demonstrated the lowest freshwater production cost at \$0.082/(L·m²). The remainder of this paper is organized as follows: Section 2 reviews the relevant literature, Section 3 describes the experimental methodology, Section 4 presents and discusses the results, and Section 5 concludes the study.

2 Literature Review

Extensive research has been conducted to optimize the rates of evaporation and condensation to improve the productivity of solar stills. A comprehensive review by Najaf and Aslan [8] confirms that enhancement strategies can be broadly categorized into two primary approaches: increasing the evaporation rate by raising the basin water temperature and promoting the condensation rate by decreasing the glass cover temperature.

2.1 Strategies for Enhancing Evaporation

Many researchers have focused on intensifying the evaporation process by increasing the saline water temperature within the solar still. One common method is incorporating heat storage materials. Sibagariang et al. [9] utilized palm shells to maintain water temperature during periods of low solar radiation, which increased freshwater output by 10–39%. The use of a corrugated absorber plate by Ghandourah et al. [10] was also shown to maximize the surface area for solar energy absorption, leading to increased thermal energy and a higher freshwater yield.

Another prevalent approach is the integration of solar stills with external heating systems. Taamneh et al. [11] employed a spiral tube collector, while Essa et al. [12] utilized internal and external mirrors to raise the water temperature. Ahmed et al. [13] used a parabolic concentrator, increasing water production by 35.6%. More directly related to the present study, Fathy et al. [14] and Al-Harahsheh et al. [15] demonstrated that coupling a solar still with a flat-plate collector effectively elevates the seawater temperature, which positively impacts the evaporation rate and total distillate yield. Other heat storage and transfer methods, such as using salt balls and sponges by Hussein et al. [16], or an integrated solar box cooker by Anggappan et al. [17], have also proven successful in increasing basin temperature and productivity.

2.2 Strategies for Enhancing Condensation

Efforts to improve the condensation process generally focus on reducing the temperature of the glass cover. Tareemi et al. [18] specifically investigated the effect of cover cooling and reported a significant productivity increase of up to 59.46%. Various cooling methods have since been explored. Elmaadawy et al. [19] employed low-cost glass coolers to improve overall effectiveness, while Kabeel et al. [20] and Kabeel and Abdelgaied [21] investigated integrated water-cooling systems. Their analyses revealed that reducing the glass cover temperature directly leads to an enhancement in freshwater flow. Building on these findings, Sharshir et al. [22] investigated the energy performance of solar stills equipped with cooling mechanisms and concluded that this method consistently maintains a lower glass temperature compared to SSCs.

2.3 Research Gap and Novelty of the Present Study

The foregoing literature review clearly indicates that efforts to improve solar still productivity have largely followed two distinct paths. However, a fundamental shortcoming of previous studies is their tendency to focus on only one of these aspects, either evaporation or condensation, rather than optimizing both simultaneously. To the best of the authors' knowledge, no prior research has investigated the simultaneous integration of an active cooling mechanism on the glass cover with the addition of a solar collector for water heating in a double-slope solar still configuration. Water is considered one of the most effective cooling mediums due to its wide availability, safety, and favorable thermal properties [23, 24]. Therefore, the primary innovation of this study lies in the concurrent application of these two strategies, which is hypothesized to create a greater temperature differential between the water surface and the glass cover, thereby significantly enhancing distillate productivity.

3 Methods

3.1 System Description

Three double-slope solar stills were constructed and tested for this investigation. Each still was fabricated from 2 mm thick iron sheets with a basin area of 1.0 m × 1.0 m. The basin walls had an edge height of 0.2 m and a central height of 0.5 m. The interior of the basin was coated with black paint to maximize solar energy absorption [25, 26]. A 5 mm thick glass cover was positioned over the basin at an inclination of 30°. This angle was selected because the tilt angle is a critical parameter for maximizing solar radiation capture and overall system performance, a principle fundamental to the efficiency of solar thermal devices [27–29]. A rubber gasket was placed between the basin and

the glass cover to ensure a proper seal and prevent vapor leakage. Finally, the exterior of the still was insulated and clad with 4 mm thick plywood.

The three configurations, depicted in Figure 1, were as follows:

• The SSCs, this unit, shown in Figure 1a, served as the baseline for comparison and operated without any modifications.

• The solar still with cover cooling (SST1), this configuration, shown in Figure 1b, incorporated a cover cooling system. A 2.5 cm diameter pipe with holes drilled 3 cm apart was mounted along the top ridge of the glass cover. A pump powered by a photovoltaic (PV) panel circulated cooling water from a reservoir, allowing it to flow over both sloped surfaces of the glass. The water was then collected by 5 cm diameter pipes at the bottom edges and returned to the reservoir in a closed loop.

• SST2, this configuration, shown in Figure 1c, included both the cover cooling system of SST1 and an external flat-plate solar collector. The solar collector, measuring 1.0 m × 1.6 m, was used to preheat the seawater from the basin. It consisted of a black-painted zinc plate and copper piping, enclosed within a double-glass casing and insulated with rockwool. A separate PV-powered DC pump circulated seawater from the basin, through the solar collector, and back into the western side of the basin in a continuous closed loop. The seawater circulation to the solar collector commenced at 10:00 AM each day.

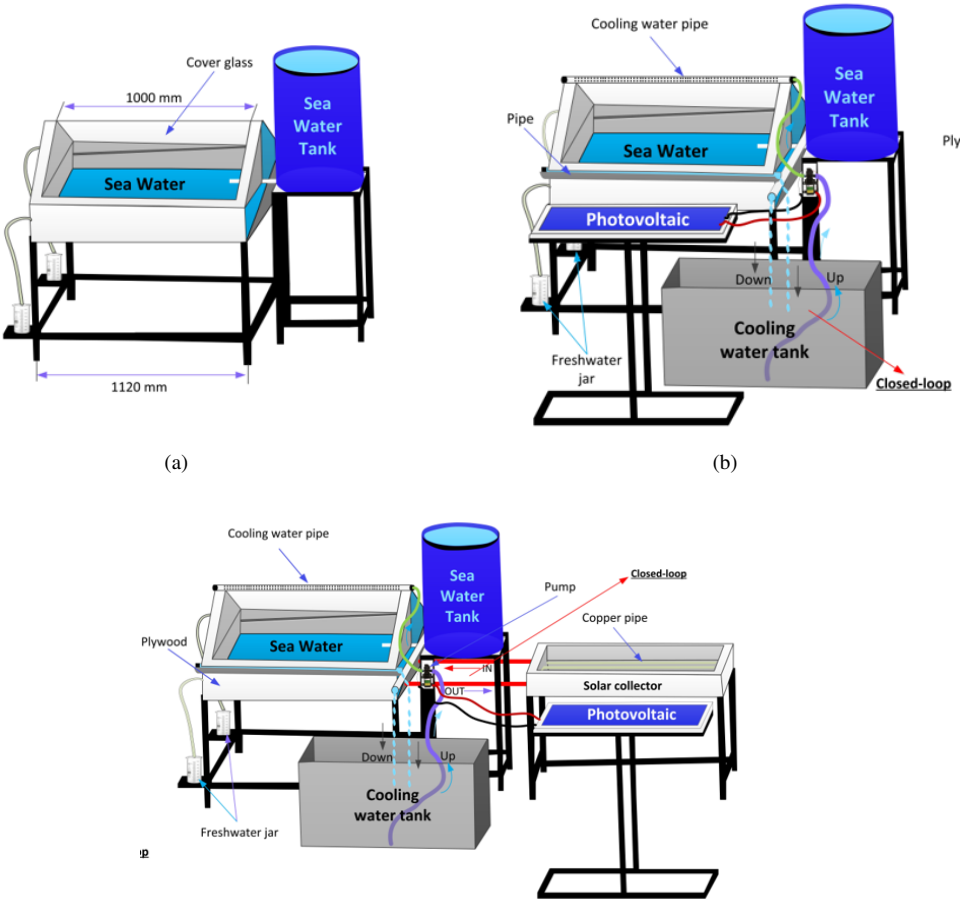

Figure 1. Solar still description: (a) SSC; (b) SST1; (c) SST2

3.2 Instrumentation and Data Acquisition

All three solar stills were equipped with a comprehensive set of instruments to monitor their performance. J-type thermocouples were used to measure the temperatures of the glass cover, basin water, absorber plate, and the moist air inside the still, as well as the ambient air temperature. An external pyranometer was used to measure global solar irradiance. The mass of the produced freshwater was measured using a digital scale. The specifications and calculated uncertainty for each instrument are detailed in Table 1. The experiments were conducted simultaneously on the rooftop of the Mechanical Engineering Building at Universitas Sumatera Utara, Indonesia (Latitude: $3°47'3.4908''$

N, Longitude: 98°41′39.1956″ E), ensuring identical environmental conditions for all three stills (Figure 2). Data was recorded daily from 8:00 to 17:00. Temperatures were logged every 5 minutes, solar irradiance every 1 minute, and the cumulative mass of fresh water was recorded every 15 minutes.

Table 1. Uncertainty of measuring instruments

Measuring Instrument	Accuracy	Range	Percent Error	Uncertainty
J type thermocouples	0.1°C	0–750°C	± 2%	0.0577°C
Pyranometer	5 W/m²	0–1500 W/m²	± 5%	2.8867 W/m²
Mass scale	2 g	0–2000 g	± 2%	1.1547 g

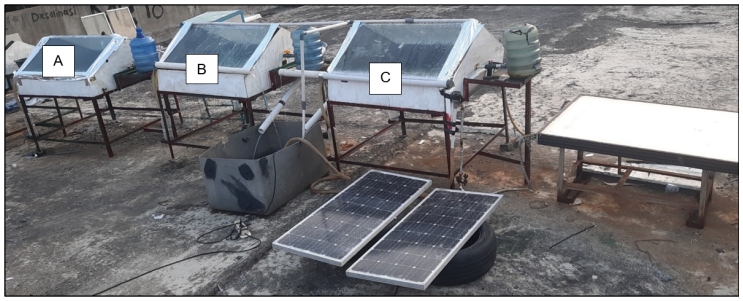

Figure 2. Preparation of experiments: (a) SSC; (b) SST1; (c) SST2

3.3 Data Analysis

The performance of the solar stills was evaluated through energy, economic, and uncertainty analyses [30, 31]:

3.3.1 Energy efficiency

The daily energy efficiency (η) of a solar still is the most critical parameter for evaluating its thermal performance. It is defined as the ratio of the energy utilized for the evaporation of water to the total solar radiation incident on the basin area over a day. This was calculated using the well-established formula [32].

$$\eta_{th} = \frac{m_{ew} \times h_{fg}}{I(t) \times A_b \times 3600} \tag{1}$$

$$m_{ew} = \frac{q_{e,w-g}}{h_{fg}} \times 3600 = \frac{h_{e,w-g} \times (T'_w - T_g) \times 3600}{h_{fg}} \tag{2}$$

$$h_R = 2.4935 \times 10^6 \times \left[\begin{array}{l} 1 - 9.4779 \times 10^{-4} \times T_m + 13132 \\ \times 10^{-7} \times T_m - 4.7974 \times 10^{-9} \times T_m^3 \end{array} \right] \tag{3}$$

where, A_b basin surface of area.

The instantaneous thermal—efficiency η_i of the solar still is described as follows:

$$\eta_i = \frac{q_{ew}}{q_w} \tag{4}$$

where, q_{ew} energy evaporation, q_w energy absorbed by water.

3.3.2 Economic analysis

The economic viability of the different solar still configurations was assessed by calculating the cost per liter (CPL) of fresh water produced. The analysis follows a standard life-cycle cost methodology, employing parameters such as the Capital Recovery Factor (CRF), Annual Salvage Value (ASV), and Annual Maintenance Cost (AMC). This methodology is widely used for the economic evaluation of solar energy systems [33].

$$FAC = CRF \times P \tag{5}$$

$$CRF = \frac{i(1+i)^n}{(1+i)^n - 1} \tag{6}$$

$$ASV = SSF \times S \tag{7}$$

$$SSF = \frac{i}{(1+i)^n - 1} \tag{8}$$

where, S = 0.2 $\times P$, i = 15%, n = 20 years.

$$AMC = 0.15 \times FAC \tag{9}$$

$$AC = FAC + AMC - ASV \tag{10}$$

$$C_{wp} = \frac{AC}{M_w} \tag{11}$$

3.3.3 Uncertainty analysis

An uncertainty analysis was conducted to quantify the potential errors associated with the experimental measurements, focusing on the instrumental uncertainty arising from the resolution of the measuring devices. The standard uncertainty (u) for each instrument was estimated based on its accuracy (a), assuming a uniform (rectangular) probability distribution, which is a standard approach when only the manufacturer's specified accuracy is available [9, 34]:

$$u = \frac{a}{\sqrt{3}} \tag{12}$$

where, a represents the accuracy (or resolution) of the measuring instrument.

The uncertainties for the primary measuring devices, as presented in Table 1, were calculated using this method. For instance, the J-type thermocouple has a specified accuracy of 0.1°C. The standard uncertainty for temperature measurements was therefore calculated as:

$$u_{temperature} = \frac{0.1^\circ\text{C}}{\sqrt{3}} \approx 0.0577^\circ\text{C} \tag{13}$$

A similar procedure was applied to the pyranometer (accuracy of 5 W/m^2) and the mass scale (accuracy of 2 g) to determine their respective uncertainties. These individual uncertainties contribute to the overall uncertainty of the calculated parameters, such as energy efficiency, and a summary of the instrument specifications and their calculated uncertainties is provided in Table 1.

4 Results and Discussion

4.1 Solar Radiation

Figure 3 shown a graph depicting the fluctuations in solar radiation with temperature in the environment. The intensity of solar radiation fluctuated significantly throughout the day, which is characteristic of the local tropical climate with intermittent cloud cover. From 08:00 to 08:30, solar radiation slowly increases, then decreases, before rising again until 10:00. After that, solar radiation decreases and then increases once more until 11:00. A subsequent reduction in sun radiation was noted from 11:00 a.m. to 12:10 p.m. Solar radiation begins to rise again from 12:15, reaching its peak at 12:36. After achieving this maximum point, solar radiation progressively diminishes till the day's end. The highest solar radiation recorded was 633.1 W/m^2 at 12:36. The trend from solar radiation was correlated with the temperature in the environment. The initial ambient temperature at the beginning of the experiment was 27.70°C, slowly increased until 09:00. The ambient temperature varied throughout the day in tandem with the trend of solar radiation, peaking at 35.90°C at 12:55 and then gradually declining until the end of the observation period.

4.2 Thermal Performance of Solar Stills

4.2.1 Glass cover temperature

The temperature of the glass cover is a crucial factor affecting the condensation process in a solar still, as a lower glass temperature is known to promote a higher condensation rate and, consequently, greater freshwater yield [18, 35, 36]. A lower glass cover temperature actively accelerates the rate of condensation. Figure 4 presents

graphs illustrating the glass temperatures for the three observed solar stills. There is a noticeable relationship between the glass temperatures of the three solar still units and the solar radiation trend. In particular, between 8:00 and 10:00, it was found that the east side's glass temperature was constantly greater than the west sides. This phenomenon is attributable to the initial contact of solar energy with the eastern glass surface. Generally, the glass temperature increased from 8:00 to 10:00, after which it tended to decrease in alignment with the solar radiation trend. Then, the water temperature fluctuates and increases to the peak rise, after that, it decreases until the day's end. The highest glass temperature is SSC west of 58.70℃ at 13:10, followed by SSC east of 55.20℃ at 13:10, SST2 east of 53.0℃ at 9:55, SST1 east of 52.70℃ at 09:55, SST2 west of 51.10℃ of 13:10, and SST1 west of 49.90℃ at 13:05. The time for the highest glass temperature SST1 east and SST2 east is different from the others, because the cooling water is supplied at 10:00. So that after 10:00 until it was time to end the experiment, the temperature of the eastern SST1 and eastern SST2 glass decreased after the water was cooled.

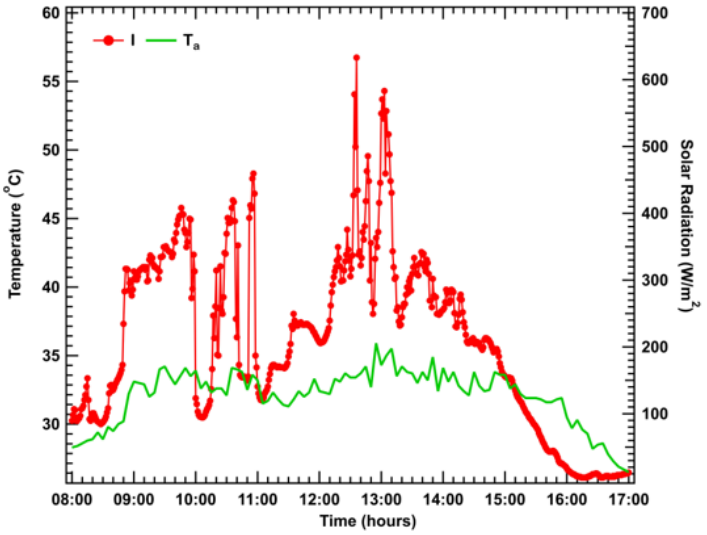

Figure 3. Solar radiation

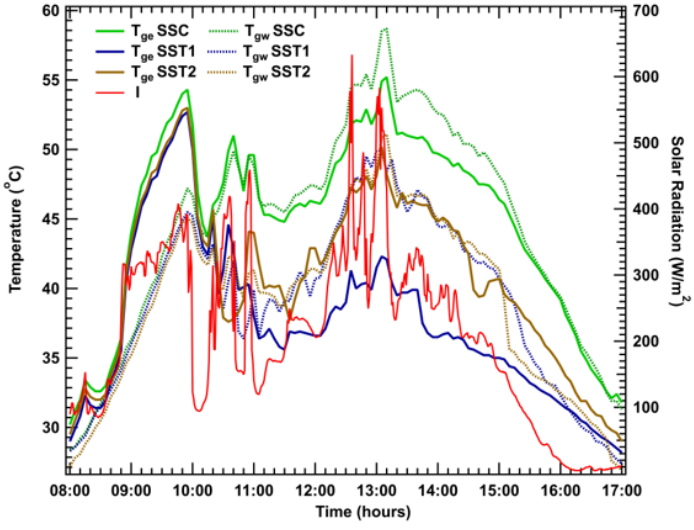

Figure 4. Glass temperature of solar stills

4.2.2 Moist air temperature

Figure 5 depicts the moist air temperature within the three solar stills. This temperature, which influences the saturation point of the air-vapor mixture, directly impacts the evaporation rate. The data shows that the moist air temperature in all units followed the solar irradiance trend. Significant differences were observed between the configurations after 10:00 AM. The SSC consistently maintained the highest moist air temperature, peaking at

55.6°C. In contrast, the SST1 recorded the lowest temperatures, peaking at only 48.0°C. This reduction is a direct consequence of the cover cooling system, which lowered the overall internal temperature of the still. The SST2, which featured both cooling and a solar collector, exhibited a moist air temperature (peak of 53.6°C) that was lower than the SSC but higher than the SST1. This intermediate temperature resulted from the competing effects of the cover cooling (which lowered the temperature) and the solar collector (which raised the water temperature, thereby increasing the temperature of the moist air above it).

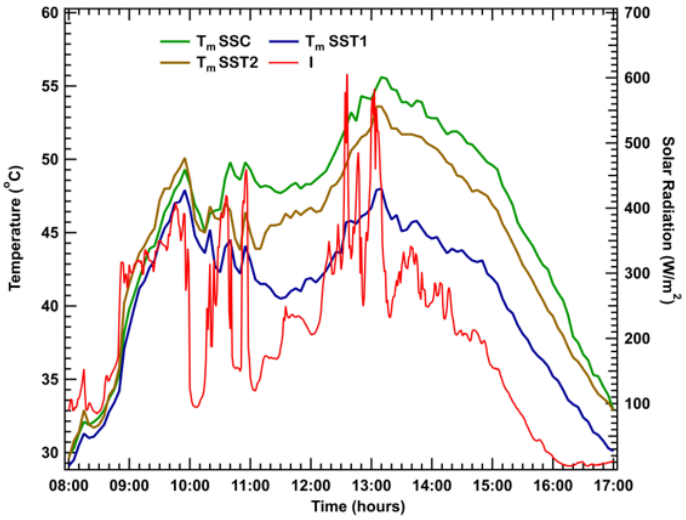

Figure 5. Moist air temperature of solar stills

4.2.3 Water temperature

Figure 6 shows the water temperature profiles of the three solar stills under investigation. The water temperature trend in the third solar still demonstrably correlates with the solar radiation pattern. Initially, water temperature rises in accordance with increasing solar radiation from 8:00 to 10:00. Subsequently, it experiences a decrease due to the corresponding decline in solar radiation. However, following this dip, the water temperature gradually increases to its peak, again aligning to overall pattern of solar radiation. This observation aligns with findings from previous research [37, 38]. After reaching their respective peaks, the water temperatures in all three solar stills progressively decrease until the end of the day, mirroring the diminishing solar radiation.

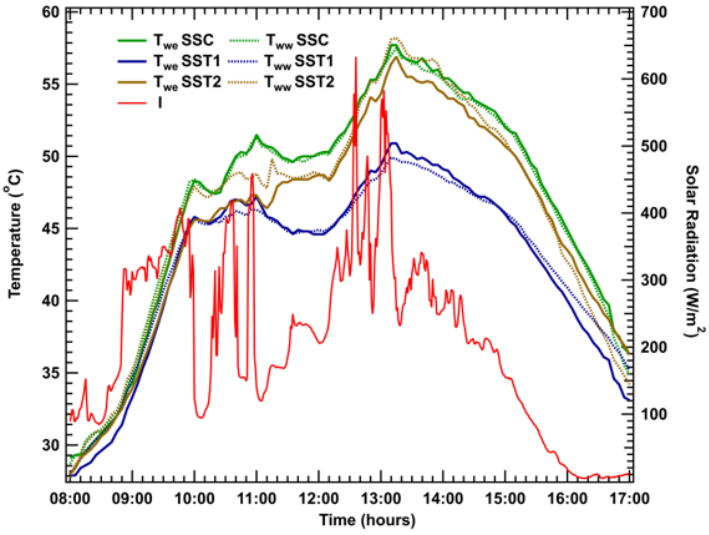

Figure 6. Water temperature of solar stills

The water temperature for the three solar stills has almost the same value from 8:00–10:00, but after that it is different because the water cooling and solar collector are used from 10:00 until day's end. The water temperature on the eastern and right sides for SSC and SST1 is almost the same. However, in SST2 the water temperature on

the western side increases due to the release of water from the solar collector into the basin occurs on that side. The highest water temperature was SST2 west of 58.2°C at 13.15, followed by SSC east of 57.7°C at 13:10, then SSC west of 57.5°C at 13:15, SST2 east at 56.9°C at 13:15, SST1 east of 50.9°C at 13:10, and SST1 west of 49.90°C at 13:10. The higher temperature observed in SST2 west compared to SST2 east is a direct consequence of the collector's water flow being discharged directly into the western side of the SST2 basin.

4.2.4 Absorber plate temperature

Figure 7 shows a graph illustrating the absorber plate temperatures for the three solar stills. The temperature trend of the absorber plates across all three units closely correlates with the trend of solar radiation. The absorber plate temperature for the three solar stills generally exhibited a gradual increase from 08:00 to 10:00, followed by a decrease, and then another rise from 10:20 until 11:00. At 11:00 a.m., was decline in solar radiation led to a corresponding decrease in the absorber plate temperatures for all three solar stills. Subsequently, temperatures gradually ascended to their peak before decreasing again until the end of the experiment. The temperatures of the three solar stills are almost the same from 08:00 to 10:00; on the other hand, the temperature difference occurs, due to absorber plates SST1 and SST2 shown lower temperatures than SSC. This divergence was attributed to the circulation of cooling water, which initially resulted in a reduction of the SST1 and SST2 glass temperatures, consequently leading to a decrease in their respective absorber plate temperatures. From 10:00 until the end of experiment, SSC consistently recorded the highest temperature, succeeded by SST2 while then SST1. The absorption plate temperature within SST2 exceeded that of SST1. This can be ascribed to the inclusion of solar collectors in SST2, which effectively elevated the seawater temperature within its basin. Furthermore, for both SST1 and SST2, the absorber plate temperature on the east side was higher than that on the west side. This observation is due to direct solar radiation impacting the eastern absorber plate from noon until the experiment's conclusion. The peak absorber plate temperatures recorded were: SSC west at 58.06°C at 13:00, SSC east at 58.0°C at 13:00, SST2 east at 57.60°C at 13:15, SST2 west at 56.5°C at 13:10, SST1 east at 53.80°C at 13:10, and SST1 west at 52.8°C at 13:10.

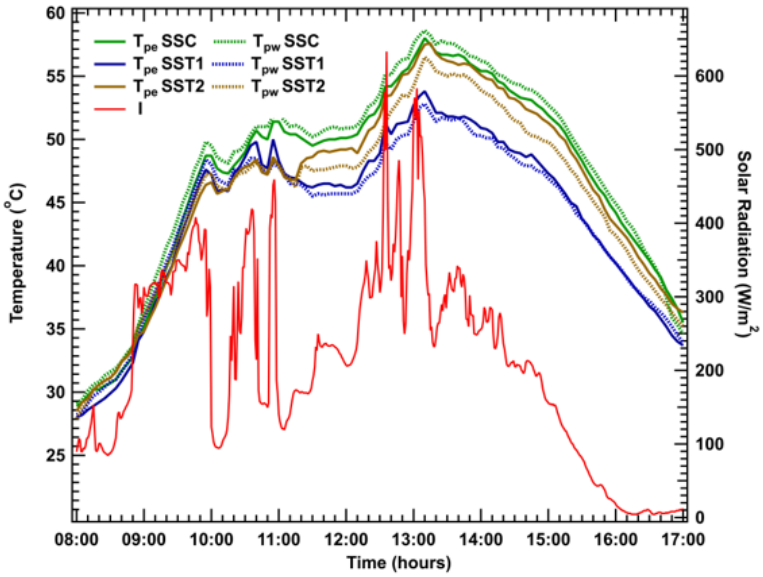

Figure 7. Plate temperature of solar stills

4.3 Freshwater Masses

4.3.1 Mass of freshwater in a 15-minute interval

Figure 8 shows a graph the mass of fresh water collected every 15 minutes for the three solar stills on the eastern and western sides. The highest freshwater mass produced every 15 minutes was calculated by SST2 west at 92 g/m^2 at 13:45, followed by SST2 east at 73 g/m^2, SST1 east at 67 g/m^2, SST1 west at 33 g/m^2, SSC east at 31 g/m^2, and SSC west at 29 g/m^2. The use of water cooling in SST1 has been shown to yield a higher mass of fresh water than the SSC. The use of water cooling and solar collectors is proven to produce a higher mass of fresh water than SST1 and SSC.

Figure 9 shows the mass of fresh water collected every 15 minutes for both the left and right sides. SSC and SST2 show same trends. The highest freshwater mass produced in 15 minutes was 161 g/m^2 by SST2 at 13:45, followed by 87 g/m^2 by SST1 at 14:30, and 60 g/m^2 by SSC at 14:00.

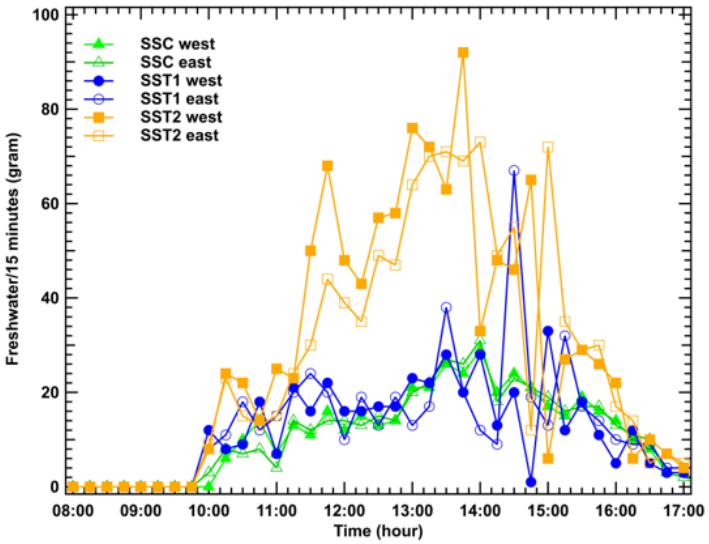

Figure 8. Mass of fresh water in a 15 minutes interval, east side and west side

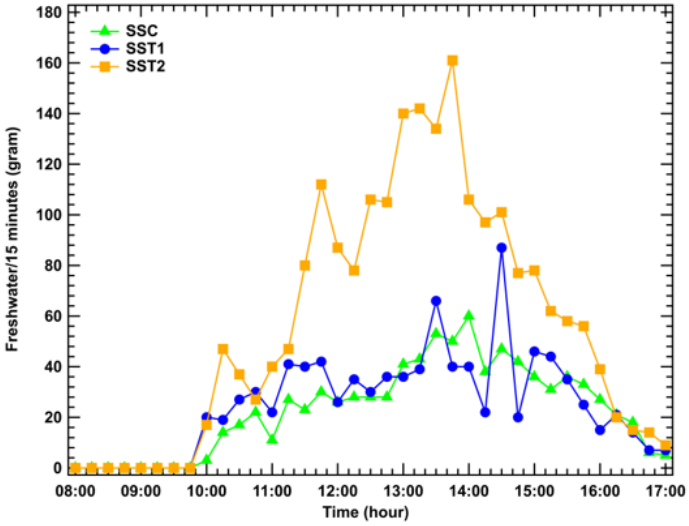

Figure 9. Mass of fresh water in a 15 minutes interval

4.3.2 Cumulative freshwater mass

Figure 10 shows a graph cumulative freshwater mass for the three solar stills on the eastern and western sides. The highest total water mass resulted by SST2 west of 1072 g/m^2 followed by SST2 east of 1020 g/m^2, followed by SST1 east of 496 g/m^2, and SST1 west of 436 g/m^2. SSC west and SSC east have the same value at the end of the test, namely 422 g/m^2.

Figure 11 shows the total cumulative water mass for the three solar stills, had the indicated trend from the start of the experiment until 11:20, but after that, SST2 increased due to the use of coolers and solar collectors. SSC and SST1 share the same trend. The highest water mass was produced by SST2 of 2092 g/m^2, followed by SST1 932 g/m^2 and SSC of 844 g/m^2. SST2 has a 147% higher mass of fresh water compared to the SSC. SST1 has a freshwater mass 10.4% higher than SSC.

While a formal comparative statistical analysis, such as ANOVA, was not performed as the experiment was conducted under the specific climatic conditions of a single day, the robustness of the findings can be inferred from the magnitude of the observed improvements relative to the measurement uncertainty. The 147% increase in freshwater productivity for SST2 compared to SSC vastly exceeds the cumulative measurement uncertainty calculated for the instruments (as detailed in Table 1). This significant margin suggests that the performance difference is a direct result of the design modifications rather than experimental artifact or random error, thereby supporting the conclusion's robustness.

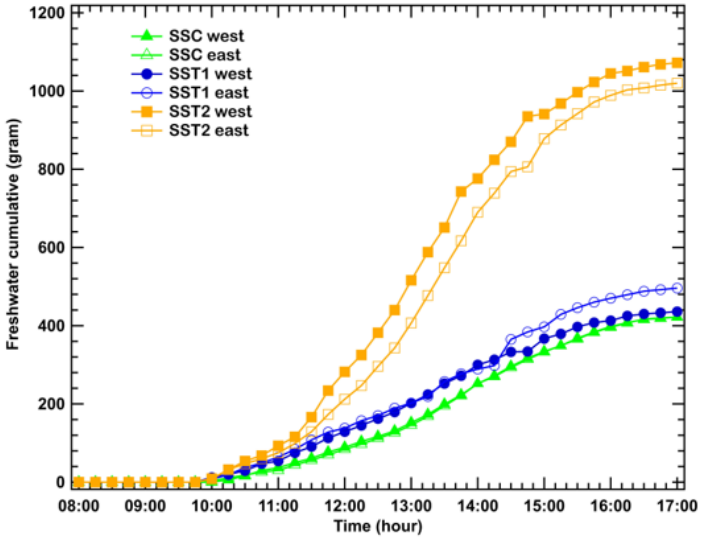

Figure 10. Cumulative freshwater mass east side and west side

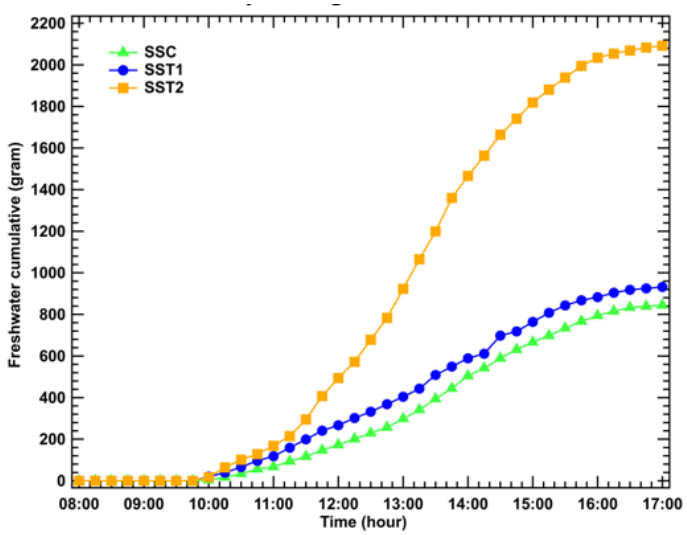

Figure 11. Cumulative freshwater mass

4.4 Performance Analysis

4.4.1 Energy efficiency

Figure 12 shows the results of energy efficiency calculations for three solar stills based on Eqs. (1)–(4). The calculated daily energy efficiencies for the three stills are shown in Figure 12. The SST2 achieved the highest energy efficiency at 44.53%, a 62.6% improvement over the SSC's efficiency of 27.38%. This superior performance is a direct result of its significantly higher freshwater yield, which indicates that a greater fraction of the incoming solar energy was effectively converted into latent heat of vaporization. Interestingly, despite producing 10.4% more water than the SSC, the SST1 exhibited a slightly lower energy efficiency of 27.27%. This apparent contradiction is due to the lower average water temperature in the SST1 basin. While the cover cooling enhanced condensation, it also increased the overall heat loss from the water to the ambient environment, thereby slightly reducing the overall thermal efficiency of the energy conversion process.

4.4.2 Economic analysis

To obtain the total cost of freshwater production, an economic analysis must be conducted. Table 2 shows the capital costs due to the construction of the three solar stills. SST2 has the highest manufacturing cost for solar stills at $344.63, followed by SST1 at $281.88, and SSC at $241.61. SST2 had the highest costs due to additional costs related to the cooling system and solar collector, but SST1 includes additional costs for the cooling system.

To obtain the total cost of freshwater production, an economic analysis must be conducted. Table 2 shows the

capital costs due to the construction of the three solar stills. SST2 has the highest manufacturing cost for solar stills at $344.63, followed by SST1 at $281.88, and SSC at $241.61. SST2 had the highest costs due to additional costs related to the cooling system and solar collector, but SST1 includes additional costs for the cooling system.

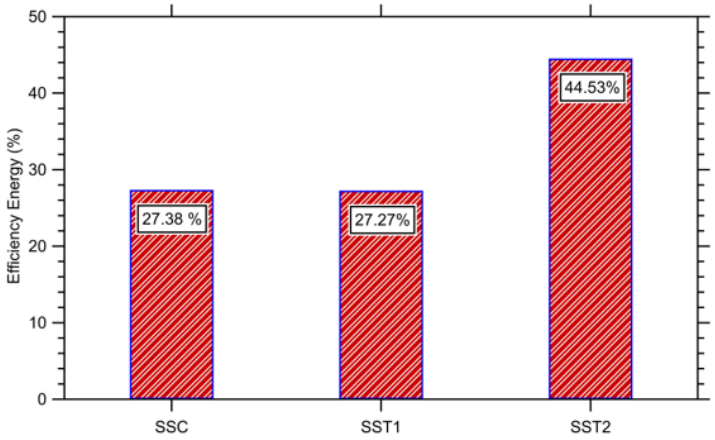

Figure 12. Energy efficiency of solar stills

Table 2. Cost of making a solar still (capital cost)

Item	SSC ($)	SST1 ($)	SST2 ($)
Absorber plate	83.89	83.89	83.89
Glass cover	20.13	20.13	20.13
Plywood	6.71	6.71	6.71
Glasswool	16.78	16.78	16.78
Angle iron	20.13	20.13	20.13
Pipe	13.42	13.42	13.42
Paint	13.42	13.42	13.42
Manufacturing costs	67.11	67.11	67.11
Cooling system		40.27	40.27
Solar collector			62.75
Total	241.61	281.88	344.63

Table 3. Cost analysis

Type	SSC	SST1	SST2
n (years)	20	20	20
i (Interest rate %)	0.15	0.15	0.15
CRF	0.16	0.16	0.16
P (Capital cost $)	241.61	281.88	344.63
S	48.32	56.38	68.93
FAC	38.60	45.03	55.06
SSF	0.01	0.01	0.01
ASV	0.47	0.55	0.67
AMC	5.79	6.76	8.26
AC	43.92	51.24	62.64
Pd (L/(m^2· day))	0.84	0.93	2.09
Py (L/(m^2·day))	308.06	340.18	763.58
CPL ($/(L·$m^2$))	0.143	0.151	0.082

Note: The abbreviations in the table are explained in the Nomenclatures

To ensure a realistic economic analysis, the key parameters were established based on local economic conditions and assumptions consistent with prior research in the region. The economic lifetime (n) of the solar still is assumed to be 20 years, a common estimate for solar thermal equipment built from durable materials. The interest rate (i)

is set at 15%. Both the lifetime and interest rate assumptions are in direct alignment with those used in a similar techno-economic study on solar stills conducted in the same geographical location Sibagariang et al. [39]. The annual maintenance cost (AMC) is estimated to be approximately 2.4% of the initial capital cost (P), which is a reasonable assumption for a low-complexity system whose primary maintenance involves routine cleaning and minor pump upkeep, reflecting local labor costs.

After calculating the capital cost, Table 3 shows the cost analysis. The cost analysis was carried out use Eqs. (5)–(11). Calculations are performed with the help of Microsoft Excel software. The lowest freshwater production cost was produced by SST2 of \$0.082/(L·m^2), followed by SSC of the \$0.143/(L·m^2) and SST1 of the \$0.151/(L·m^2). The cost of producing SST2 freshwater is lower because SST2 produces more freshwater than SSC. Meanwhile, SST1 was higher production cost of fresh water than SSC. This is due to the additional cost for the cooling system, even though it was higher mass of fresh water, the increased mass of fresh water produced in SST1 cannot cover the cost of the cooling system. Therefore, the production cost of freshwater SST1 exceeds that of SSC.

5 Conclusion

An experimental investigation of three double-slope solar still configurations—a conventional solar still (SSC), a solar still with cover cooling (SST1), and a solar still integrating both cover cooling and a solar collector (SST2)—was successfully conducted. The key conclusions drawn from this study are as follows:

1. The integrated SST2 design demonstrated a profound synergistic effect between its components, resulting in a freshwater productivity of 2092 g/m^2, a 147% increase compared to the conventional SSC (844 g/m^2).

2. The SST2 was also the most energy-efficient configuration, achieving an efficiency of 44.53%, which represents a 62.6% improvement over the SSC.

3. Despite a higher initial capital cost, the SST2 proved to be the most economically viable option, with the lowest CPL of produced water (\$0.082/(L·m^2)).

4. The SST1 configuration (cooling only), while increasing productivity by 10.4%, was not economically viable, as the modest yield increase did not offset the additional system cost.

This study rigorously demonstrates that the simultaneous integration of cover cooling and an external solar collector is a highly effective and economically sound strategy for significantly enhancing the performance of solar stills.

6 Practical Implications and Recommendations

The findings of this study offer significant practical implications for decision-makers, engineers, and organizations involved in providing sustainable freshwater solutions. The research moves beyond theoretical analysis to provide clear, data-driven recommendations for the practical implementation of solar still technology.

• Investment Justification for Enhanced Systems, the primary managerial implication is that the higher initial capital cost for an enhanced system like the SST2 (with both cooling and a solar collector) is strongly justified. While the SST1 (cooling only) offered a marginal 10% increase in yield, its production cost was higher than the conventional still, making it an economically poor choice. In contrast, the SST2's dramatic 147% increase in productivity led to the lowest CPL (\$0.082/(L·m^2)). This provides a clear directive for project managers: for new installations, investing in the fully-equipped SST2 configuration is the most cost-effective strategy to maximize water output and ensure long-term economic viability.

• Deployment in Target Regions, this research validates the SST2 design as a highly effective, decentralized water production system. It is particularly suitable for deployment in remote, coastal, and island communities that lack reliable access to electricity and centralized water infrastructure but have abundant solar irradiance and access to saline or brackish water. Policymakers and NGOs can confidently consider this technology as a robust solution to improve public health and reduce the burden of water collection in such regions.

• Socio-Economic Impact, by providing a low-cost, independent source of clean drinking water, the widespread adoption of this technology can have significant socio-economic benefits. It can enhance community resilience, improve health outcomes by reducing waterborne diseases, and free up time previously spent on water collection for education and other economic activities.

7 Study Limitations and Future Work

While this study demonstrates the significant potential of combining cooling and solar collectors, its limitations must be critically acknowledged to properly contextualize the findings.

Firstly, the geographic specificity of the experiment, conducted in Medan, Indonesia, presents a key constraint on the generalizability of the results. Medan's equatorial climate is characterized by high humidity and intermittent cloud cover, which influences both evaporation rates and incoming solar radiation. In arid or semi-arid regions with higher direct solar irradiance and lower ambient humidity, the absolute productivity of all solar still configurations would likely be greater.

Secondly, the short experimental duration of single-day tests limits the assessment of long-term applicability. The results do not capture performance variations across different seasons (e.g., monsoon vs. dry season) or the effects of material degradation over time, such as fouling in the collector pipes or degradation of the absorber plate's coating. This limitation directly impacts the economic analysis, as the assumed 20-year lifetime is a standard engineering estimate not yet validated by long-term field data for this specific hybrid design. Furthermore, the single-day duration of the experiment precluded the possibility of conducting comparative statistical analyses to formally establish the significance of the variations between the three still configurations.

Based on these limitations, several key directions for future research are recommended to build upon this work:

• Conduct long-term performance evaluations over multiple consecutive days and across different seasons to gather data for a robust statistical analysis and to validate the system's durability and economic assumptions.

• Optimize the design parameters for the SST2 system, such as solar collector dimensions, cooling water flow rate, glass tilt angle, and water depth, to maximize productivity and efficiency.

• Investigate the use of alternative materials, such as phase-change materials (PCMs) or nanofluids for the cooling medium, to further enhance performance or reduce costs.

• Develop and test scalable versions of the SST2 design in diverse geographical locations with different climatic conditions to validate the universality of the findings.

• Examine techniques to achieve a more uniform water temperature distribution within the basin of the SST2 model to optimize the evaporation effect across the entire surface area.

Author Contributions

Conceptualization, Y.P.S. and H.A.; methodology, W.S. and Y.P.S.; software, W.S.; validation, W.S.; formal analysis, W.S. and T.B.S.; investigation, T.B.S., H.A. and Y.O.; data curation, W.S. and Y.P.S.; writing review and editing, W.S., Y.P.S., H.A. and H.V.S.; visualization, T.B.S.; supervision, H.A. and Y.O. All authors have read and agreed to the published version of the manuscript.

Funding

This research was funded by the Indonesian Collaborative Research (RKI) scheme (Grant No.: 2/UN5.2.3.1/PPM/KP-RKI/2022).

Data Availability

The data used to support the research findings are available from the corresponding author upon request.

Conflicts of Interest

The authors declare no conflict of interest.

References

[1] WHO, "Drinking-water," 2023. https://www.who.int/news-room/fact-sheets/detail/drinking-water

[2] S. S. A. Toosi, H. R. Goshayeshi, I. Zahmatkesh, and V. Nejati, "Experimental assessment of new designed stepped solar still with Fe3O4+ graphene oxide+ paraffin as nanofluid under constant magnetic field," *J. Energy Storage*, vol. 62, p. 106795, 2023. https://doi.org/10.1016/j.est.2023.106795

[3] Z. Y. Ho, R. Bahar, and C. H. Koo, "Passive solar stills coupled with Fresnel lens and phase change material for sustainable solar desalination in the tropics," *J. Clean. Prod.*, vol. 334, p. 130279, 2022. https://doi.org/10.1016/j.jclepro.2021.130279

[4] A. Maghsoudian, S. Rashidi, and R. Rafee, "Solar still performance enhancement with reflectors and various shapes of absorber plates," *Appl. Therm. Eng.*, vol. 278, p. 127261, 2025. https://doi.org/10.1016/j.applthermaleng.2025.127261

[5] S. S. S. Al-Mezeini, M. A. Siddiqui, M. Shariq, T. M. Althagafi, I. A. Ahmed, M. Asif, J. A. Alsufyani, S. A. Algarni, M. B. N. A., K. M. A. Elamin, and et al., "Design and experimental studies on a single slope solar still for water desalination," *Water*, vol. 15, no. 4, p. 704, 2023. https://doi.org/10.3390/w15040704

[6] C. Phukapak and S. Phukapak, "Experimental study of the effect of water depth on the productivity of double basin solar stills in seawater desalination," *Appl. Sci. Eng. Prog.*, vol. 9, no. 1, pp. 11–18, 2016. https://doi.org/10.14416/j.ijast.2015.12.004

[7] Z. Arifin, N. F. Alfaiz, S. D. Prasetyo, W. B. Bangun, and M. A. M. Rosli, "Techno-economic evaluation of hybrid solar-wind power plant for generating electricity at toll merak rest area electric vehicle charging station," *Int. J. Energy Prod. Manag.*, vol. 9, no. 4, pp. 247–254, 2024. https://doi.org/10.18280/ijepm.090405

[8] F. Najaf and S. R. Aslan, "Enhancing water purification in solar stills through incorporation of renewable energy technology: An experimental study on the efficiency and cooling mechanisms—A review," *Int. J. Heat Technol.*, vol. 42, no. 1, pp. 101–110, 2024. https://doi.org/10.18280/ijht.420111

[9] Y. P. Sibagariang, F. H. Napitupulu, H. Kawai, and H. Ambarita, "Study on the effect of oil palm shells on fresh water productivity of double slope solar still," *J. Energy Storage*, vol. 70, p. 108000, 2023. https://doi.org/10.1016/j.est.2023.108000

[10] E. Ghandourah, H. Panchal, O. Fallatah, H. M. Ahmed, E. B. Moustafa, and A. H. Elsheikh, "Performance enhancement and economic analysis of pyramid solar still with corrugated absorber plate and conventional solar still: A case study," *Case Stud. Therm. Eng.*, vol. 35, p. 101966, 2022. https://doi.org/10.1016/j.csite.2022.101966

[11] Y. Taamneh, A. M. Manokar, M. M. Thalib, A. E. Kabeel, R. Sathyamurthy, and A. J. Chamkha, "Extraction of drinking water from modified inclined solar still incorporated with spiral tube solar water heater," *J. Water Process Eng.*, vol. 38, p. 101613, 2020. https://doi.org/10.1016/j.jwpe.2020.101613

[12] F. A. Essa, A. S. Abdullah, Z. M. Omara, A. E. Kabeel, and Y. Gamiel, "Experimental study on the performance of trays solar still with cracks and reflectors," *Appl. Therm. Eng.*, vol. 188, p. 116652, 2021. https://doi.org/10.1016/j.applthermaleng.2021.116652

[13] M. M. Ahmed, F. Alshammari, I. Alatawi, M. Alhadri, and M. Elashmawy, "A novel solar desalination system integrating inclined and tubular solar still with parabolic concentrator," *Appl. Therm. Eng.*, vol. 213, p. 118665, 2022. https://doi.org/10.1016/j.applthermaleng.2022.118665

[14] M. Fathy, H. Hassan, and M. S. Ahmed, "Experimental study on the effect of coupling parabolic trough collector with double slope solar still on its performance," *Sol. Energy*, vol. 163, pp. 54–61, 2018. https://doi.org/10.1016/j.solener.2018.01.043

[15] M. Al-Harahsheh, M. Abu-Arabi, M. Ahmad, and H. Mousa, "Self-powered solar desalination using solar still enhanced by external solar collector and phase change material," *Appl. Therm. Eng.*, vol. 206, p. 118118, 2022. https://doi.org/10.1016/j.applthermaleng.2022.118118

[16] A. K. Hussein, M. E. H. Attia, H. J. Abdul-Ammer, M. Arıcı, M. B. B. Hamida, O. Younis, R. Z. Homod, and A. Abidi, "Experimental study of the impact of low-cost energy storage materials on the performance of solar distillers at different water depths," *Sol. Energy*, vol. 257, pp. 221–230, 2023. https://doi.org/10.1016/j.solener.2023.04.013

[17] G. Angappan, S. Pandiaraj, A. J. Alrubaie, S. Muthusamy, Z. Said, H. Panchal, V. P. Katekar, A. E. Shoeibi, and A. E. Kabeel, "Investigation on solar still with integration of solar cooker to enhance productivity: Experimental, exergy, and economic analysis," *J. Water Process Eng.*, vol. 51, p. 103470, 2023. https://doi.org/10.1016/j.jwpe.2022.103470

[18] A. A. Tareemi and S. W. Sharshir, "Performance improvement of double-slope solar still using locally sourced sand, coupled with glass cooling integration," *Results Eng.*, p. 105166, 2025. https://doi.org/10.1016/j.rineng.2025.105166

[19] K. Elmaadawy, A. W. Kandeal, A. Khalil, M. R. Elkadeem, B. Liu, and S. W. Sharshir, "Performance improvement of double slope solar still via combinations of low cost materials integrated with glass cooling," *Desalination*, vol. 500, p. 114856, 2021. https://doi.org/10.1016/j.desal.2020.114856

[20] A. E. Kabeel, S. W. Sharshir, G. B. Abdelaziz, M. A. Halim, and A. Swidan, "Improving performance of tubular solar still by controlling the water depth and cover cooling," *J. Clean. Prod.*, vol. 233, pp. 848–856, 2019. https://doi.org/10.1016/j.jclepro.2019.06.104

[21] A. E. Kabeel and M. Abdelgaied, "Enhancement of pyramid-shaped solar stills performance using a high thermal conductivity absorber plate and cooling the glass cover," *Renew. Energy*, vol. 146, pp. 769–775, 2020. https://doi.org/10.1016/j.renene.2019.07.020

[22] S. W. Sharshir, M. A. Rozza, A. Joseph, A. W. Kandeal, A. A. Tareemi, F. Abou-Taleb, and A. E. Kabeel, "A new trapezoidal pyramid solar still design with multi thermal enhancers," *Appl. Therm. Eng.*, vol. 213, p. 118699, 2022. https://doi.org/10.1016/j.applthermaleng.2022.118699

[23] Z. M. Omara, A. S. Abdullah, A. E. Kabeel, and F. A. Essa, "The cooling techniques of the solar stills' glass covers—A review," *Renew. Sustain. Energy Rev.*, vol. 78, pp. 176–193, 2017. https://doi.org/10.1016/j.rser.2017.04.085

[24] S. Shoeibi, N. Rahbar, A. A. Esfahlani, and H. Kargarsharifabad, "Energy matrices, exergoeconomic and enviroeconomic analysis of air-cooled and water-cooled solar still: Experimental investigation and numerical simulation," *Renew. Energy*, vol. 171, pp. 227–244, 2021. https://doi.org/10.1016/j.renene.2021.02.081

[25] A. Negi, R. P. Verma, A. Saxena, L. Ranakoti, P. Bhandari, T. Singh, and G. N. Tiwari, "Design and performance of black painted Khes wick modified solar still: An experimental and 5E analysis," *Int. J. Thermofluids*, vol. 20, p. 100491, 2023. https://doi.org/10.1016/j.ijft.2023.100491

[26] A. Mohan, J. U. Prakash, and A. M. Manokar, "Performance analysis of conventional solar still and solar still with crab shells as energy storage material," *J. Energy Storage*, vol. 126, p. 117071, 2025. https://doi.org/10.1016/j.est.2025.117071

[27] H. Ş. Aybar and H. Assefi, "Simulation of a solar still to investigate water depth and glass angle," *Desal. Water Treat.*, vol. 7, no. 1-3, pp. 35–40, 2009. https://doi.org/10.5004/dwt.2009.692

[28] R. S. Hansen and K. K. Murugavel, "Enhancement of integrated solar still using different new absorber configurations: An experimental approach," *Desalination*, vol. 422, pp. 59–67, 2017. https://doi.org/10.1016/j.desal.2017.08.015

[29] S. M. A. M. Reda, M. A. M. Hussein, J. M. Hadi, H. A. Al-Asadi, K. A. Hammoodi, S. K. Ayed, and H. S. Majdi, "Optimizing tilt angle for thermal efficiency of vacuum tube solar collectors," *Int. J. Energy Prod. Manag.*, vol. 9, no. 1, pp. 57–64, 2024. https://doi.org/10.18280/ijepm.090107

[30] G. N. Tiwari and A. T. Shyam, "Energy systems in electrical engineering handbook of solar energy theory," *Anal. Appl.*, 2016.

[31] H. N. Singh and G. N. Tiwari, "Monthly performance of passive and active solar stills for different Indian climatic conditions," *Desalination*, vol. 168, pp. 145–150, 2004. https://doi.org/10.1016/j.desal.2004.06.180

[32] L. S. Hyal, J. M. Jalil, and A. O. Hanfesh, "Numerical and experimental study of a single-slope solar still integrated with wick material and external condenser," *Int. J. Heat Technol.*, vol. 42, no. 4, pp. 1359–1374, 2024. https://doi.org/10.18280/ijht.420426

[33] F. Hosseinifard, M. Salimi, and M. Amidpour, "Evaluating economic feasibility and machine learning-driven prediction for solar still desalination in Iran," *Results Eng.*, vol. 25, p. 103823, 2025. https://doi.org/10.1016/j.rineng.2024.103823

[34] M. S. B. Jahromi, V. Kalantar, H. S. Akhijahani, H. Kargarsharifabad, and S. Shoeibi, "Performance analysis of a new solar air ventilator with phase change material: Numerical simulation, techno-economic and environmental analysis," *J. Energy Storage*, vol. 62, p. 106961, 2023. https://doi.org/10.1016/j.est.2023.106961

[35] H. AbdelMeguid and W. M. El Awady, "Optimizing solar still performance through glass cover optical properties: A mathematical modeling and theoretical investigation," *Ain Shams Eng. J.*, vol. 15, no. 3, p. 102589, 2024. https://doi.org/10.1016/j.asej.2023.102589

[36] A. A. Salman, A. H. Al-Abbas, and H. M. Majid, "Experimental and numerical analysis for the performance of a solar desalination still with M-shaped glass cover design," *Int. J. Heat Technol.*, vol. 43, no. 4, pp. 1418–1428, 2025. https://doi.org/10.18280/ijht.430419

[37] A. Maghsoudian, S. Rashidi, and R. Rafee, "Solar still performance enhancement with reflectors and various shapes of absorber plates," *Appl. Therm. Eng.*, vol. 278, p. 127261, 2025. https://doi.org/10.1016/j.applthermaleng.2025.127261

[38] H. A. N. Diabil, H. G. Hameed, A. Al-Manaa, and A. Alahmer, "Enhancing solar still productivity and efficiency using external condensers and a copper pipe solar collector," *Therm. Sci. Eng. Prog.*, vol. 62, p. 103652, 2025. https://doi.org/10.1016/j.tsep.2025.103652

[39] Y. P. Sibagariang, O. A. Rosyid, H. Ambarita, A. Sudrajat, M. R. Ridlo, N. M. Lande, M. Hason, and A. Fudholi, "Solar still double slope evaporation improvement using palm kernel as sensible heat storage material," *Case Stud. Therm. Eng.*, vol. 66, p. 105705, 2025. https://doi.org/10.1016/j.csite.2024.105705

Nomenclature

A_b	Area of the basin (m^2)
a	Accuracy of the measuring instrument
AC	Annual of Cost ($/year)
AMC	Annual Maintenance Cost ($/year)
ASV	Annual Salvage Value ($/year)
CPL	Cost per liter of produced water $\left(\mathrm{L}/\mathrm{m}^2\right)$
CRF	Capital Recovery Cost
FAC	Fixed Annual Cost ($/year)
h_{fg}	Latent heat of vaporization of water (J/kg)
h_{ew}	Evaporative heat transfer coefficient from water (W/(m^2·K))
$I_{(t)}$	Total solar radiation intensity (W/m^2)
i	Interest rate (%)
m_{ew}	Mass flow rate of evaporated water (Kg/s)
n	Economic life of the system (years)

P	Capital cost ($)
$\mathrm{P_d}$	Daily freshwater productivity (L/(m²·day))
$\mathrm{P_y}$	Annual freshwater productivity (L/(m²·year))
q_{ew}	Evaporation energy (W/m²)
q_w	Energy absorbed by water (W/m²)
S	Salvage value ($)
SSF	Sinking Fund Factor
T_g	Temperature glass (K or °C)
T_w	Water temperature in the basin (K or °C)
T_a	Ambient temperature (K or °C)
u	Standard uncertainty

Greek symbols

n_{th}	Thermal efficiency (%)

Subscripts

a	Ambient
b	Basin
ew	Evaporated water
g	Glass
s	Solar/absorbed
th	Thermal
w	Water